IEEE Access
Multidisciplinary ⋮ Rapid Review ⋮ Open Access Journal

Received 24 October 2023, accepted 2 November 2023, date of publication 8 November 2023,
date of current version 16 November 2023.

Digital Object Identifier 10.1109/ACCESS.2023.3331388

RESEARCH ARTICLE

A Wideband Broadside Coupled Yagi Antenna and Arrays System for Ku Band Applications

MUHAMMAD NASIR[1], ADNAN IFTIKHAR[1], (Senior Member, IEEE), SYED MUZAHIR ABBAS[2], (Senior Member, IEEE), RASHID SALEEM[3], MUHAMMAD FARHAN SHAFIQUE[1], (Senior Member, IEEE), AND MOATH ALATHBAH[4]

[1]Electrical and Computer Engineering Department, COMSATS University Islamabad, Islamabad Campus, Islamabad 45550, Pakistan
[2]Faculty of Science and Engineering, School of Engineering, Macquarie University, Sydney, NSW 2109, Australia
[3]Department of Telecommunication Engineering, University of Engineering and Technology (UET) Taxila, Taxila, Punjab 47050, Pakistan
[4]Department of Electrical Engineering, College of Engineering, King Saud University, Riyadh 11451, Saudi Arabia

Corresponding authors: Adnan Iftikhar (adnaniftikhar@comsats.edu.pk) and Moath Alathbah (malathbah@ksu.edu.sa)

This work was supported in part by the Researchers Supporting Project, King Saud University, Riyadh, Saudi Arabia, under Grant RSPD2023R868; and in part by the National Research Program for Universities (NRPU) offered by Higher Education Commission (HEC) of Pakistan under Project 8196.

ABSTRACT This work presents a novel and highly compact broadband Yagi antenna structure in multilayer configuration for Ku band applications. The antenna is formed by stacking two identical Yagi elements which are fed in-phase with a single strip-based transmission line. Metalized vias has been used to connect the ground planes and to launch the signal in the driver element of both Yagi elements. The design has multiple advantages of providing large gain, large impedance bandwidth, high front-to-back ratio along with low radiation leakage. The unique broadside coupling introduced in this topology causes constructive interference of near fields in the H-plane thus causing wider HPBW. Detailed optimization processes along with physical insight have been provided for a better understanding of the working principle. The design has been extended into a 1×4 antenna array formation in the E-plane to enhance the boresight gain. The array thus formed offers a fractional bandwidth of 26.6% over the frequency range from 16.51 GHz to 21 GHz. It produces a gain of 11.83 dBi with a front-to-back ratio of 33.2 dB. The HPBW in the H-plane is measured to be 94.7° which allows this antenna system to be used in cellular communication, scanning, and surveillance system.

INDEX TERMS Broadside coupled Yagi pair, front-to-back ratio, 3-dB beamwidth, antenna array.

I. INTRODUCTION

Antenna beamwidth is a major design factor that influences the choice of antenna being used. Especially in cellular communication, the beamwidth is restricted as per specification in order to avoid inter-cell interference. However, at the same time, a large gain and high Font-to-Back (F/B) ratio is also desired for system optimal performance. In the design of such an antenna system, the elevation beamwidth is often not given much importance, however larger elevation beamwidth can allow deeper coverage into the cell with high signal strength. Thus, antenna systems with constrained beamwidth in the azimuth plane and large beamwidth in the elevation plane can play a significant role in overall communication system performance. The major drawback associated with the conventional parabolic reflector or horn antennas is their bulkiness since other associated applications like surveillance, security, and traffic monitoring require compact antennas. Traveling wave antennas are decent and the required beamwidth performance nonetheless, they have an inherent limitation of narrow bandwidth. Thus, there is a tradeoff between bandwidth and beamwidth as far as traveling wave antennas are concerned.

Among various choices, Yagi-Uda antenna can be a suitable option for these types of applications owing to their large gain, low profile structure, and better efficiency [1],

The associate editor coordinating the review of this manuscript and approving it for publication was Mohammad Zia Ur Rahman.

[2], [3]. Nevertheless, the practical use of the Yagi-Uda antennas which is a class of travelling wave antenna is hindered by their narrow bandwidth due to the parasitic arrays in the geometry and use of microstrip transmission lines for the excitation. On the contrary, other classes of travelling wave antennas such as Vivaldi or log-periodic antennas inherently possess wide bandwidth. Also, the miniaturization requirement associated with planar antennas necessitates a tight placement of the radiating structure and feeding network which ultimately compromises the bandwidth, radiation performance, and beamwidth features, especially in the case of arrays. Multilayer topology, on the other hand, is an effective strategy for achieving design compactness through the separate realization of the feed network and radiating structure on the several substrate layers with different thicknesses. This method not only results in a low-profile design but also produces a broad impedance bandwidth and more importantly addresses the associated requirements of miniaturization.

Various designs have been reported in the literature, which are realized in multilayer configurations with directors on one layer and feeding sections placed on another layer [4], [5], [6], [7], [8], [9], [10]. Kramer et.al. [5] etched parasitic directors on a different substrate layer in the vertical direction to obtain a broadside radiation pattern and customized gain by increasing the number of directors in the vertical direction. This vertical loading of the director is practical at mm-wave due to smaller wavelengths; however, this strategy may be impractical for the lower frequency range. Similarly, in [6], vertical stacking of the directors on the separate dielectric layers having air gaps between the layers resulted in an overall height of about 0.7 λ_0 (50 mm) at 4.2 GHz. In [7], a 5.8 GHz stacked Yagi antenna is proposed where each layer is separated with an air gap hence resulting in an overall height of 0.56 λ_0 (29 mm) at 5.8 GHz. In another work, a 10-layered folded dipole antenna as a driven element and a rectangular loop-shaped patch as a director is presented [8]. The compact design offered a peak gain of 5.67 dBi and a 3-dB beamwidth of 125° at 28 GHz in the azimuth plane. A 10-layered Quasi-Yagi antenna demonstrated in [9] for mobile handsets utilized multiple through vias to establish RF connectivity between the vertically stacked loop-shaped directors and partial vias for the common ground. The design offers a bandwidth of 12.3 % with a gain of 5.51 dBi at 28 GHz, however, the incorporation of multiple vias increases the overall design complexity. In addition, at 28 GHz, a four-element array based on a 10-layered unit element provided a narrow bandwidth of 12.3 % and a modest gain of 9.98 dBi. The elevation and azimuth plane 3-dB beamwidths recorded were 23° and 114°, respectively. A bowtie dipole driver with one edge directly connected to a UWB balun, through an eight-layer probe feed, produced a fractional bandwidth of 102.8 % from 3.4 GHz to 10.6 GHz and a maximum gain of 13 dBi at 10.6 GHz [10].

It is observed that the F/B ratio and cross-polarization level requirements of a printed Yagi-Uda antenna, being critical parameters for directional communications, are not addressed in [5], [6], [7], [8], [9], and [10]. Whereas in [11] an antenna structure is proposed having multiple microstrip patches arranged in the front of an inset-feed patch driver to achieve a high F/B ratio (up to 15 dB). Fractional bandwidth of 10 % is demonstrated with a gain of 10.7 dBi at 5.2 GHz. Furthermore, in another study, a design of a 7-element planar Yagi structure is proposed that offered a cross-polarization level of ≤ -16 dBi over a 22 GHz – 26 GHz band with a gain variation of 9 – 11 dBi [12].

The literature review clearly elucidates that the vertical placement of the Yagi antennas and their arrays have only been realized by placing directors in the vertical directions and therefore are incapable of providing wide elevation beamwidth along with a high F/B ratio. On top of that, these stacked configurations pose significant limitations in terms of vertical extensions at microwave frequencies. The stacked designs with an air gap between layers are bulky and impractical for most compact installations. The design with a high F/B ratio often has low fractional bandwidth and polarization purity. Thus, it is challenging to design an antenna system that offers a high F/B ratio and wide fractional bandwidth with sufficient gain and polarization purity. To address the aforementioned challenges, a novel antenna system is proposed that comprises a pair of broadsides coupled Yagi antennas fed through a strip line section with a bowtie feeding element and three directors each. To ensure ruggedness and physical stability commercial prepregs have been used between the layers. Once the unit element of Broadside Coupled Yagi Pair (BCYP) is designed, a four-element array based on the unit radiator is realized to enhance directivity and F/B ratio with wide beamwidth.

II. DESIGN EVOLUTION

The geometrical configurations of the BCYP shown in Figure 1 (a) were initially designed by modeling a planar bowtie driver element, instead of a conventional dipole, to achieve a wide impedance bandwidth [13], [14]. The length of the bowtie driver was empirically estimated using (1) by considering 0.254 mm thick Roger 4350B substrates ($\varepsilon_{sub1} = 3.66$, $tan\delta = 0.0037$ and 0.1 mm thick Bondply 4450 ($\varepsilon_{prepreg} = 3.54$, $tan\delta = 0.004$) for dominant TM_{01} mode resonant frequency [15], [16], [17].

$$L_3 = \frac{c}{2.5 f_r \sqrt{\varepsilon_{sub1} + \varepsilon_{prepreg}}}. \tag{1}$$

where, ε_{sub1} and $\varepsilon_{prepreg}$ are respective dielectric constants of the substrates and prepregs. f_r is the resonant frequency and c being the speed of light. Eq. (1) resulted in an estimated value of L_3 as 2.05 mm at 22.6 GHz (0.15 λ_0). Instead of adding a reflector element on the back of the driver element and imposing a requirement of a balun which limits the impedance matching bandwidth, a ground plane acting as a reflector is placed on the top of the substrate, and the other arm of the bowtie driver is attached to it. The vertical separation of the two arms of the bowtie element is 0.608 mm

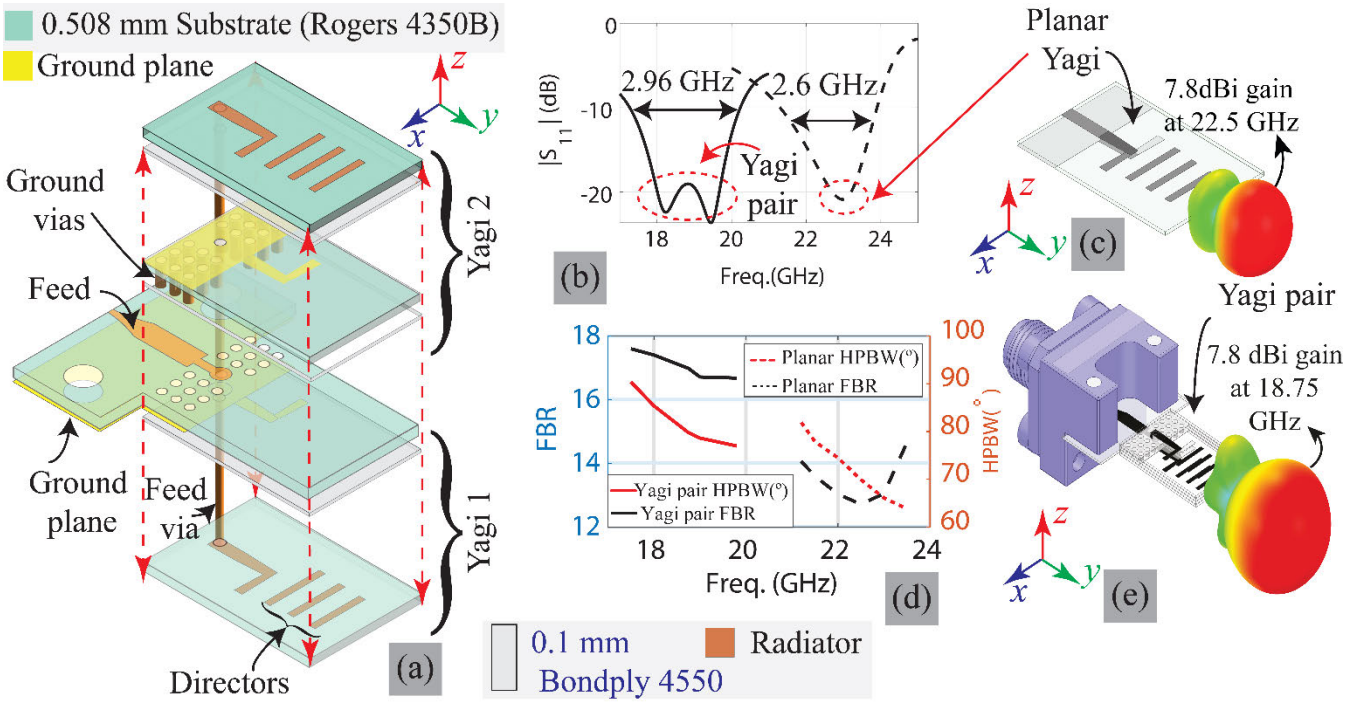

FIGURE 1. (a) An Exploded view of the proposed broadside coupled Yagi pair. (b) Impedance bandwidth comparison of the single Yagi and broadside coupled Yagi pair. (c) 3D radiation pattern at 22.5 GHz. (d) F/B Ratio and HPBW comparison. (e) 3D radiation pattern at 18.75 GHz.

(0.508 mm thick substrate and 0.1 mm thick prepreg). The ratio of tapered widths of the bowtie driver was estimated using (2) by considering the realizable widths [16], [17].

$$\frac{w_3}{w_2} = \frac{0.25\lambda_r}{\sqrt{\varepsilon_{sub1} + \varepsilon_{prepreg1}}}. \tag{2}$$

where, w_3 and w_2 are the opening and closing width of the bowtie driver respectively.

Finally, three directors having lengths of 0.8 λ_g, 0.75 λ_g, and 0.73 λ_g are added sequentially as parasitic elements with interspacing of 0.3 λ_g, at 22.23 GHz [7]. The insertion of the directors resulted in a frequency-dependent mutual coupling among the directors and the driver which played a significant role in gain optimization. Additionally, the radiation properties in the end-fire direction can also be controlled by optimizing the director and driver separation.

This optimization of the directors and reflector lengths along with a uniform spacing of 1.5 mm (0.3 λ_g) resulted in an impedance bandwidth of 2.6 GHz from 21.3 GHz to 23.9 GHz. Once the antenna elements are optimized another Yagi element with the same geometry is placed underneath, as shown in Figure 1 (a). The antenna structure now comprises a pair of Yagi elements that are broadside coupled. The whole antenna structure is fed through a microstrip to strip-line section that feeds both bowtie drivers with an in-phase signal through a via hole [18], [19]. The strip-line feed also ensures low radiation leakage and a large F/B ratio. A 3D radiation pattern, illustrating end-fire radiation characteristics and a gain of 7.8 dBi for both the single element and the pair, is depicted in Figure 1 (c). The radiation performance of the single and Yagi pair antenna configurations in terms of 3-dB beamwidth and F/B ratio are shown in Figure 1 (d).

TABLE 1. Optimized dimensions (in mm) of the final layout.

Parameters	Values	Parameters	Values
W	8	ω_3	0.561
L	12	ω_4	0.45
L_1	1.8	ω_5	0.34
L_2	2.5	ω_6	1.5
L_3	2.05	ω_7	0.55
L_4	3.6	d_1	1.2
L_5	2.5	d_2	0.6
ℓ_3	3.65	d_3	0.6
ω_1	0.85	d_4	1.65
ω_2	0.614	Lg_1	6.1
ℓ_1	4	ℓ_2	3.75

The design achieved the overall antenna dimensions of 8 × 12 × 2.3 mm^3 (excluding the external footprint of the feeding section). The impedance matching results in Figure 1 (b) clearly show that the vertical stacking of the Yagi pair, having the same dimensions as that of the planar Yagi, procreated a fractional bandwidth of 15.8 % from 17.27 GHz to 20.23 GHz. Whereas the single Yagi offers 11.5 % fractional bandwidth from 21.3 GHz to 23.9 GHz. The shifting of the operating band to a lower frequency also shows the compactness achieved after stacking a Yagi pair.

The broadside coupling introduced between the two Yagi elements also improved the F/B ratio as well as HPBW

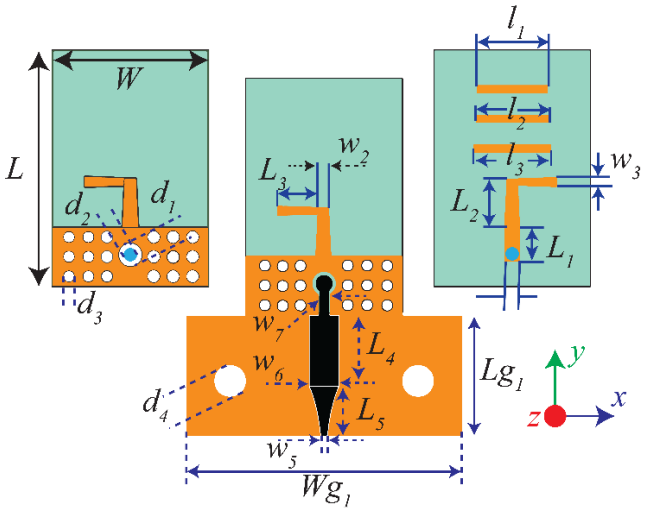

FIGURE 2. Description of the geometrical parameters of the broadside coupled Yagi pair.

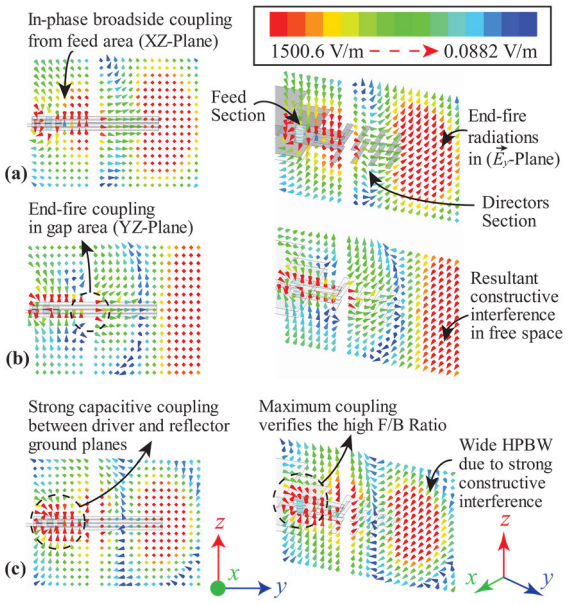

FIGURE 3. Cross-sectional and isometric view of the E-fields vector plot on the proposed structure at (a) 17.5 GHz, (b) 18.75 GHz, (c) 19.8 GHz for the validation of broadside capacitive coupling from feed to the driven elements through a metallic via.

in the elevation plane (H plane) as shown in Figure 1 (d). 3D radiation characteristics of the single Yagi and Yagi pair are shown in Figure 1 (c) and (e), respectively. The coupling gap (g) between the Yagi pair was mathematically estimated using (3) [7].

$$g \approx \frac{c}{f\sqrt{\varepsilon_T}} \times \frac{1}{4\sqrt{h_{TS} + h_{TP}}} \tag{3}$$

$$\varepsilon_T = \varepsilon_{sub} + \varepsilon_{prepreg} \tag{4}$$

where ε_T is the sum of the relative permittivity of included substrates ε_{rs} and prepregs ε_{rp}, while h_{TS} and h_{TP} are the total thickness of the substrates and prepregs, respectively. The modeling and simulations of the structure were carried out in the 3D full wave electromagnetic simulator Ansys v. 2021 [20]. The details of the dimensional parameters of the proposed BCYP are shown in Figure 2, whereas corresponding finalized dimensional values are listed in Table 1.

A. EMBEDDED STRIP-LINE FEED CONFIGURATION AND WORKING PRINCIPLE

It can be observed from the E-field vector analysis shown in Figure 3 that the strip-line feed excites both the radiators in-phase and couples the EM wave towards the directors of both Yagi elements simultaneously. The vertical separation of much smaller than a wavelength in both the Yagi elements (upper and lower) enables in-phase EM wave propagation and causes constructive interference at the radiating edge attributing to a large F/B ratio and better directivity [19].

The in-phase propagation is also evident from the cross-sectional view of the E-field vector plots at 17.5 GHz, 18.75 GHz, and 19.8 GHz as shown in Figures 3 (a), (b), and (c), respectively. The constructive interference of the E-field vectors in stacked configuration also reveals that the optimized separation between the directors and the driver is responsible for the desired optimum coupling and little radiation leakage. This optimum separation can be estimated using (3); however, the radiation characteristics may slightly change in the Yagi pair configuration due to shorter wavelength and substrate losses at higher frequencies. The broadside capacitive coupling from the strip-line feed can also be viewed from the vector analysis of the E-field distribution shown in Figure 3. Furthermore, to elaborate on the working principle, radiation mechanism, and wide bandwidth feature of the proposed BCYP, the current analysis is also presented at different frequencies. It can be observed in Figure 4 that uniform separation of the strip-line feed and driver elements on both sides induces equal phase currents in both elements. The Yagi pair concentrates current at the same positions, as shown in Figures 4 (a – d). Equal magnitudes of the current density can be observed at both driver elements at 17.5 GHz. Whilst the current density is concentrated on directors for 18.75 GHz, 19 GHz, and 19.8 GHz due to progressive phase variation for different frequencies, as depicted in the top, bottom, and isometric views shown in Figures 4 (b – d), respectively. Therefore, it can be inferred from the current distribution analysis that multiple resonances, due to variable lengths of the directors and mutual coupling between directors, result in a wide impedance bandwidth [11].

An isometric view of the current distribution analysis depicted in Figure 4 (a – d) also illustrates that the proposed feeding mechanism ensured minimal back or sidewise radiation as no leakage current is seen in the ground plane and all current density is localized under the feeding strip. Therefore, the embedded strip-line feed not only reduces the overall antenna size but also reduces unwanted radiation from the feed due to the presence of the ground plane on its top and bottom.

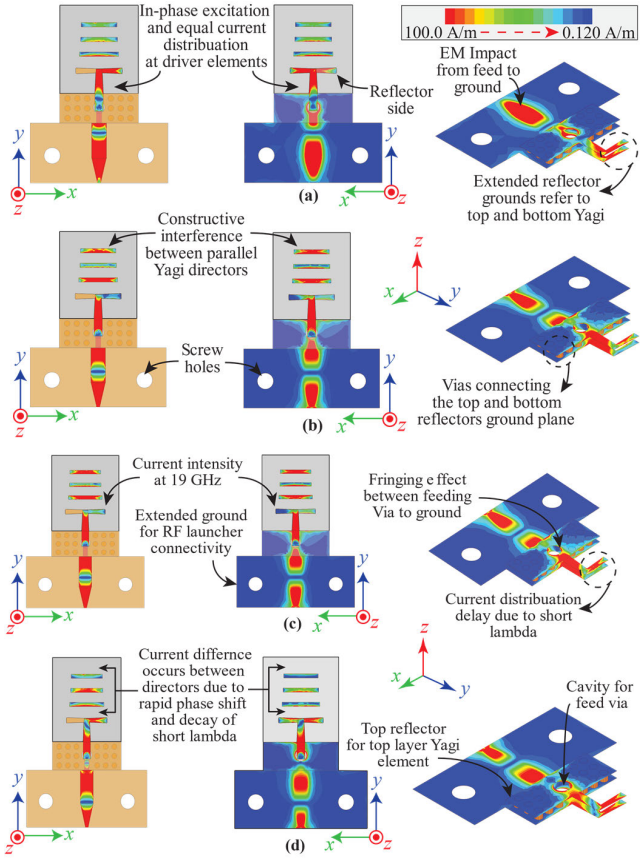

FIGURE 4. Current distribution analysis of the BCYP at different frequencies. The left plot shows the top Yagi element, the middle plot shows the bottom element, and the right plot shows the isometric view of the ground plane (a) 17.5 GHz (b) 18.75 GHz (c) 19.8 GHz.

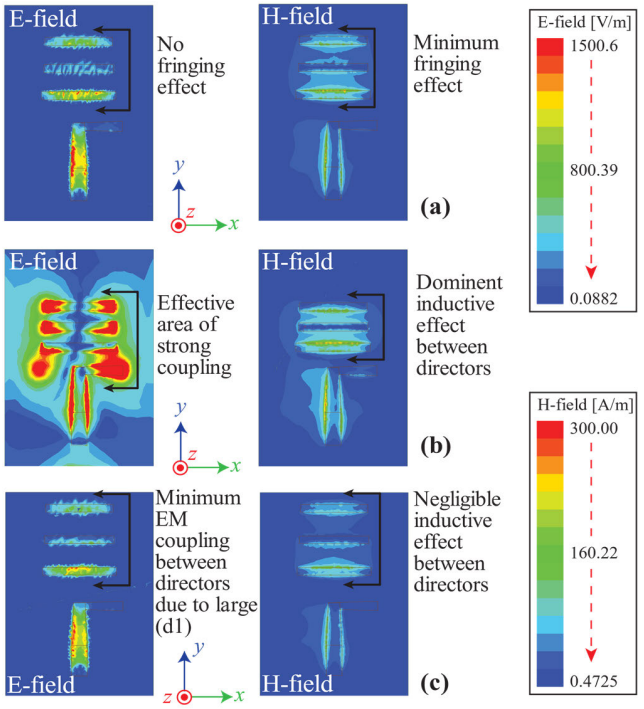

FIGURE 5. E-field and H-field distribution analysis for EM coupling with different values of d_1 (a) 0.1 λ_h (Proposed BCYP) (b) 0.075 λ_h (c) 0.125 λ_h at higher frequency (20.23 GHz).

III. PARAMETRIC ANALY SIS OF THE PROPOSED BCYP

The parametric analysis of the proposed BCYP is also carried out on the geometrical parameters that influence the gain, F/B ratio, and beamwidth. The parameters that cause significant variation in the response are related to the separation and lengths of the directors. Therefore interspacing (d_1) between the directors, length of directors (l_1, l_2, l_3), and the gap between the two Yagi elements (g) has been investigated.

A. INTERSPACING OF DIRECTORS

The director's separation has a major impact on the beamwidth, F/B ratio, and gain due to the variation in mutual coupling between them. When a parasitic element is placed closer to the driven element, the gap capacitance as well as the near field coupling form the radiation beam increased. However, there exists a lower limit of spacing to avoid the coupling from fringing fields of the director. This phenomenon is depicted in Figure 5. In Figure 5 (a), for optimized spacing ($d_1 = 0.1\lambda_h$), sufficient inductive coupling and gap capacitance can be observed that leads to optimized F/B ratio and gain. On the other hand, for $d_1 = 0.075\lambda_h$, (Figure 5 (b)) strong inductive and capacitive coupling is visible causing performance deterioration. Likewise, a larger gap of $d_1 = 0.125\lambda_h$ (Figure 5 (c)) weakens the desired critical coupling levels again compromising the antenna performance.

The effect of inter-director spacing relative to higher frequency wavelength (λ_h) on gain and HPBW is plotted in Figure 6 (a) for the three separation cases of critically coupled, over-coupled, and under-coupled. It can be observed that decreasing the distance between the directors decreases the gain of the antenna but increases HPBW as a convention. This effect of varying d_1 on gain and HPBW is caused by the variation in the EM strengths, as elaborated in Figure 5 (a – c).

The F/B ratio of the antenna is also largely influenced by directors' spacing as plotted in Figure 6 (b). At $0.125\lambda_h$ a 20dB F/B ratio is attained because the bowtie driver concentrates the EM fields towards directors, which is also supported by the ground plane reflector that inhabits the flow of back radiation. In contrast, the existence of the dominant inductive effect due to the lesser inter-director gap results in higher back radiation causing the reduction in the F/B ratio.

B. LENGTH OF DIRECTORS

The electrical lengths of the directors also play an important role in optimizing antenna gain, beamwidth, and F/B ratio by varying the coupled field intensity. The directors' lengths are chosen in a log-periodic fashion to concentrate maximum fields in the end-fire direction. With the increase in the length of directors, the effective radiation area increases causing an enhancement in the gain. However, as the length approaches

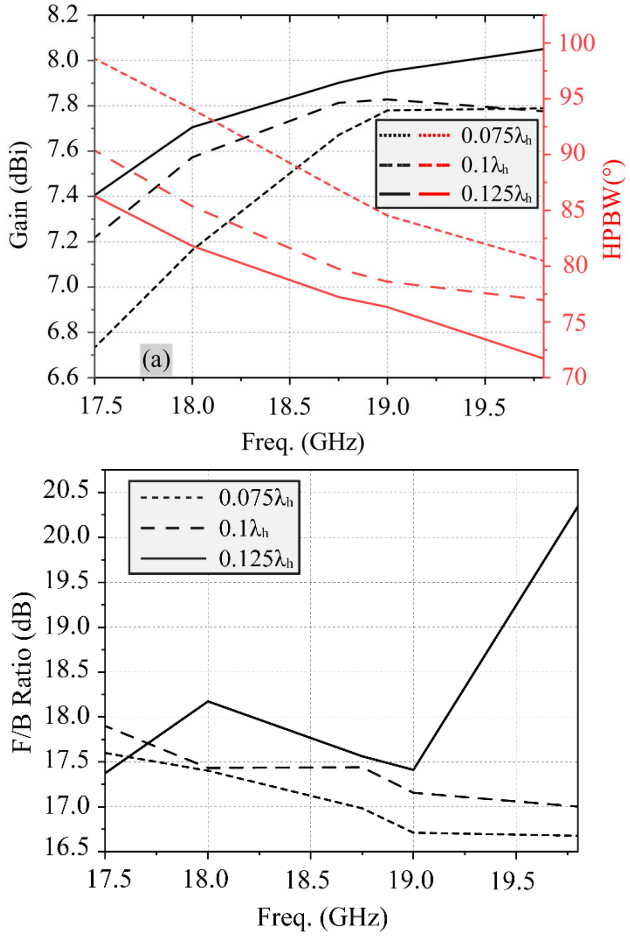

FIGURE 6. (a) Effect of d_1 on gain and HPBW of the proposed BYCP. (b) Parametric analysis of d_1 to observe its impact on the F/B ratio.

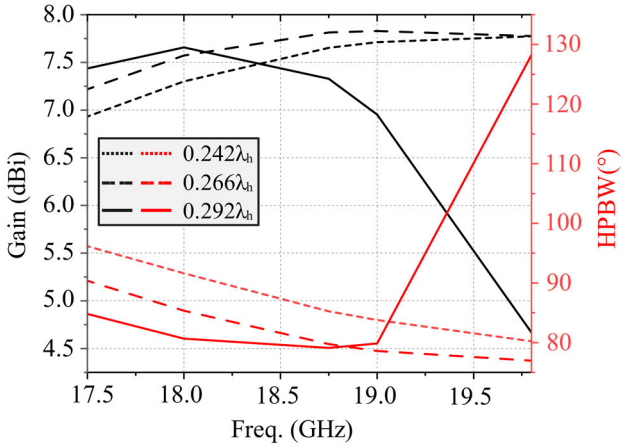

FIGURE 7. Parametric analysis on the length of the directors to observe variations in the gain and HPBW.

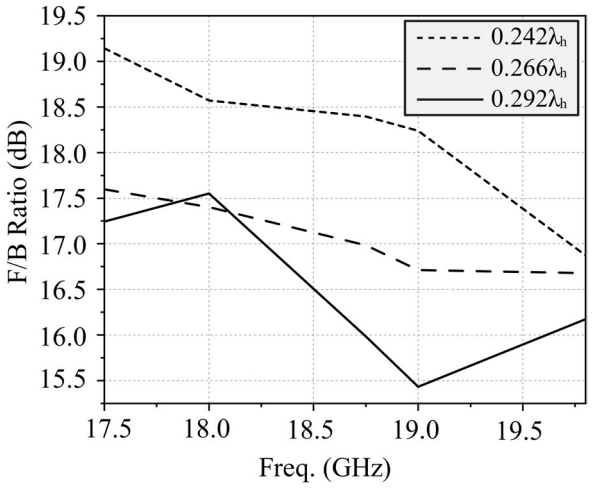

FIGURE 8. Change in F/B ratio w.r.t the length of the directors.

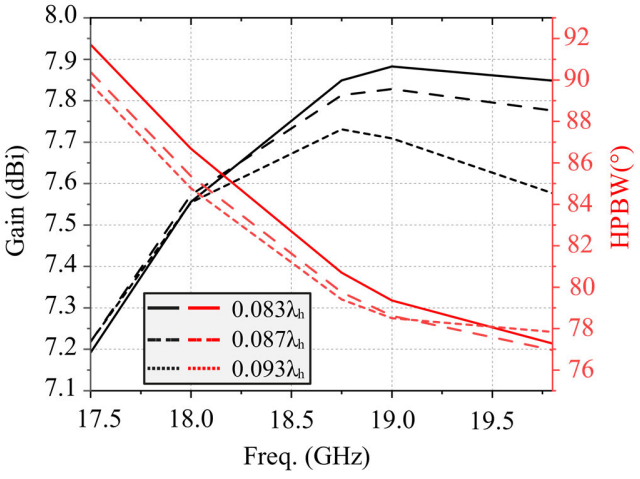

FIGURE 9. Parametric analysis of g and its effect on the gain and HPBW.

the driver's length the gain reduces and consequently the HPBW increases mainly because of the dominance of the back radiation. Therefore, the length of the directors should be kept smaller than that of the driver. Figure 7 illustrates the variation of the HPBW and gain with reference to the director's length. It can be observed that as soon as the director's length becomes comparable to the bowtie driver element ($0.31\lambda_h$), the gain drops rapidly. The length of directors is directly proportional to the gain and inversely proportional to the HPBW as long as they are shorter than the driver element. Similarly in Figure 8 it can be observed that larger lengths reduce the F/B ratio, thus the upper limit of the director's length is guided by the F/B ratio and the lower limit of the length is directed by the antenna gain and HPBW.

C. VARIATION SEPARATION (g)

The vertical separation (g) between the top and bottom Yagi elements directly affects the beamwidth, gain, and F/B ratio. This parameter is vital as it ensures the in-phase feeding of both elements as well as ascertains the critical broadside E field coupling between them. In addition, the separation gap (g) also plays an important role in reducing the radiation leakages on the sides owing to the inherent pure TEM mode propagation property of the strip-line feeds. The broadside spacing of the two Yagi elements is varied from

0.083 λ_h - 0.093 λ_h to analyze its effect on gain and HPBW, as shown in Figure 9. It is clear that for optimum spacing of 0.083 λ_h, tight coupling is more pronounced resulting in lower radiation leakage, and maximum gain is achieved.

Additionally, the optimum separation gap between the Yagi elements reinforced the constructive interference at the radiation edge that caused gain enhancement. Impedance bandwidth was also found to be increasing with the increase in the gap but the weak coupling causes gain deterioration.

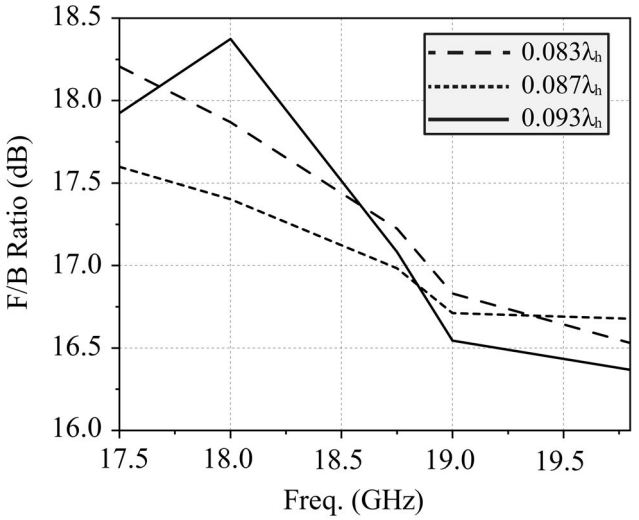

FIGURE 10. Effect on F/B ratio w.r.t change in the vertical distance (*g*) between the Yagi pair.

The HPBW of the H-plane is directly influenced by this gap as seen from Figure 9. A larger gap reduces HPBW, especially at lower frequency bands. The F/B ratio is also dependent on the separation of the Yagi pair, as shown in Figure 10. Larger separation provides a better F/B ratio at the lower frequencies on account of larger wavelength that generates tighter coupling, however, F/B ratio's declining trend appears at the higher frequencies.

IV. FABRICATION AND MEASURED RESULTS OF SINGLE ELEMENT BCYP

The final geometry of the BCYP, shown in Figure 1 (a), was fabricated to experimentally validate the antenna performance. The proposed BCYP design fabrication was carried out by first milling the relevant conducting patterns of the driver and directors on the respective layers using LPKF S103 milling machine, as depicted in the exploded view shown in Figure 1 (a). Initially, only the middle two layers were laminated together with the help of 4450B prepreg and hydraulic hot press.

Once bonded, the ground via holes were machined and metalized through LPKF Pro Conduct system to ensure the connectivity of the two ground planes. After curing the conductive epoxy, the top and bottom layers were added to the substrate stack using prepregs and the heated press. Once the lamination was completed, the central signal via hole

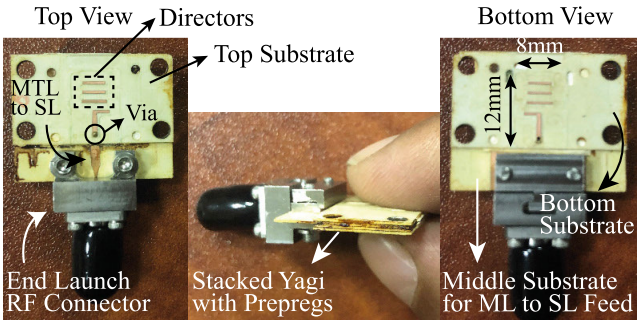

FIGURE 11. Photographs of the fabricated BCYP. SL feed is embedded between the top and bottom structures, whereas the middle substrate is extended to attach the RF launcher.

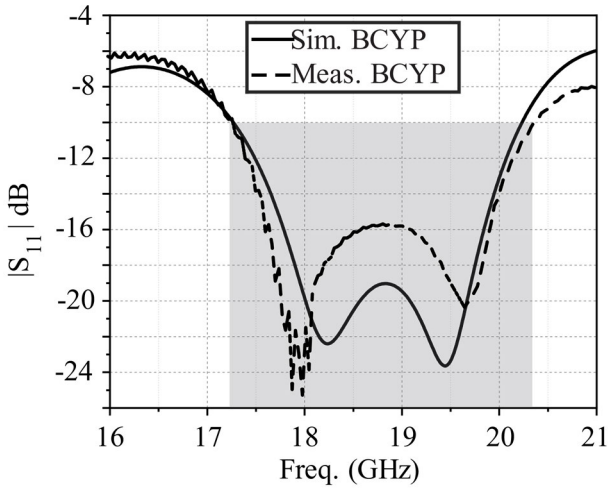

FIGURE 12. Simulated and measured reflection coefficient of the proposed BCYP.

was machined and metalized to finish the construction of the design. The finalized manufactured BCYP prototype is shown in Figure 11, whereas a 2.92 mm RF end launch connector (Model # 1092–01A–5) [21] was used to connect the antenna with the VNA for the measurements. The measured results of the magnitude of the reflection coefficient are depicted in Figure 12. It can be observed from the measured results that the proposed BCYP has wide impedance bandwidth ($|S11| < -10$ dB) of 2.8 GHz starting from 17.0 GHz to 19.8 GHz. The response is slightly shifted towards lower frequency which is primarily caused by potential fabrication imperfections and slight possible misalignment of the dielectric layers as the process was carried out manually.

The radiation pattern of the proposed BCYP was also measured in a fully anechoic chamber to observe the far-field behavior of the fabricated prototype. The E- and H-plane radiation pattern measurements were performed by mounting the prototype on the turntable in horizontal and vertical positions, respectively, as depicted in Figure 13.

A standard broadband horn antenna (Model # LB-20265) [22] is used as a transmitter in the far-field range. The corresponding results of E- and H-plane (at 17.5 GHz and

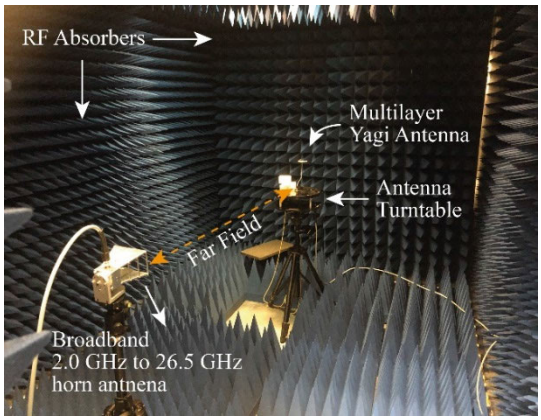

FIGURE 13. A picture captured during the radiation pattern measurement of the BCYP prototype in the anechoic chamber.

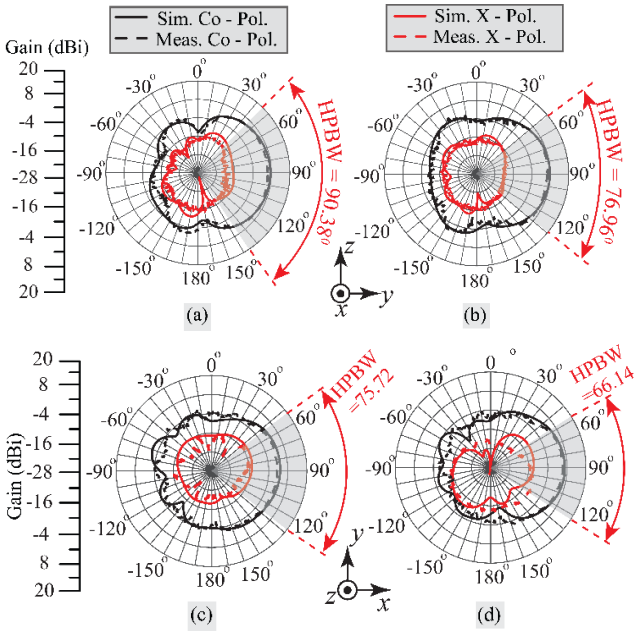

FIGURE 14. Comparison of measured and simulated Co – and Cross (X) – polarization components (a) H – plane at 17.5 GHz, (b) H – plane at 19.8 GHz, (c) E – plane at 17.5 GHz, and (d) E – plane at 19.8 GHz.

19.8 GHz) with their co- and cross- (X) polarization components are plotted in Figure 14 (a) – (d). The results comparison between simulated and measured results shown in Figure 14 also verified that the proposed BCYP has end-fire radiation patterns. The X-polarization components in the E- and H-plane are around −16 dBi at 17.5 GHz and 19.8 GHz. The measured HPBW in the H-plane is 90.38° at 17.5 GHz and 76.96° at 19.8 GHz respectively. This broader HPBW is the result of strong broadside capacitive coupling which is achieved by using multilayer topology in the Yagi antenna. The reduction in the HPBW at higher frequencies is complemented by the increase in the gain. For instance, at 19.8 GHz, the measured gain value is 7.76 dBi, as compared to the gain at the lower frequency (17.5 GHz) which is 7.25 dBi, as shown in Figure 15.

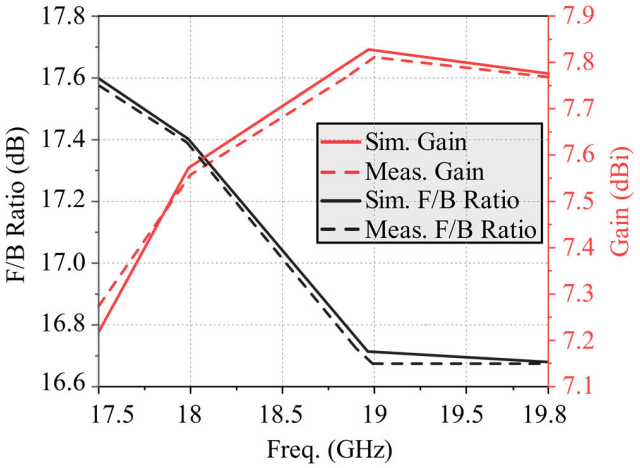

FIGURE 15. Comparison between simulated and measured boresight Gain (dBi) and F/B (dB) values over the entire band of interest.

A comparison of simulated and measured F/B ratio values is also plotted in Figure 15. It can be observed that the F/B ratio varies between 16.6 dB to 17.6 dB and these high values are achieved because of well confined EM fields between the Yagi pair. The optimum reflecting ground plane also contributes to the improvement of the F/B ratio.

V. DESIGN, ANALYSIS, AND REALIZATION OF 1 × 4 BCYP ARRAY

In order to demonstrate the capability of the BCYP in an array formation to achieve a higher gain in the E- plane (azimuth) sector antennas and airborne applications, an antenna array of 1 × 4 elements have been investigated. The array is formed by placing the four identical BCYP antennas with a separation of $\lambda_0/2$ (9.1 mm at lowest frequency) in the E-plane. The half wavelength separation at the lowest frequency ensured minimum sidelobe levels. A microstrip corporate feed mechanism is designed for compactness and in-phase excitation of the array elements. The feeding section has been optimized to achieve the maximum possible impedance bandwidth ($|S_{11}| \leq -10$ dB). The in-phase excitation of the signal through the feeding network can be seen in the current distribution plot in Figure 16 (a).

The 3D radiation pattern that remains in the end-fire direction can be seen in Figure 16 (a). For experimental validation of the 1 × 4 element array, a prototype was realized and measured as shown in Figure 16 (b). The measured and simulated reflection coefficient is plotted in Figure 16 (c) and a wide impedance bandwidth of 5.08 GHz ranging from 16.51 GHz to 21. 60 GHz can be observed.

The layout of the array along with the details of the quarter wave impedance matching in the feeding section is depicted in Figure 17. The measurements of the far-field radiation having E- and H-planes along with their co- and cross-(X) polarization components are plotted in Figure 18. An evident end-fire behavior of the radiation pattern is observable in Figure 18. The X-polarization components in both E- and

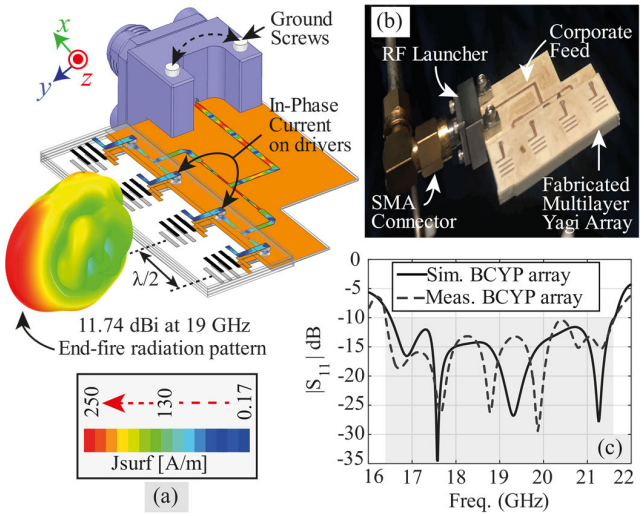

FIGURE 16. 1 × 4 array formation (a) Isometric view with current distribution (b) fabricated prototype (c) Reflection coefficient comparison.

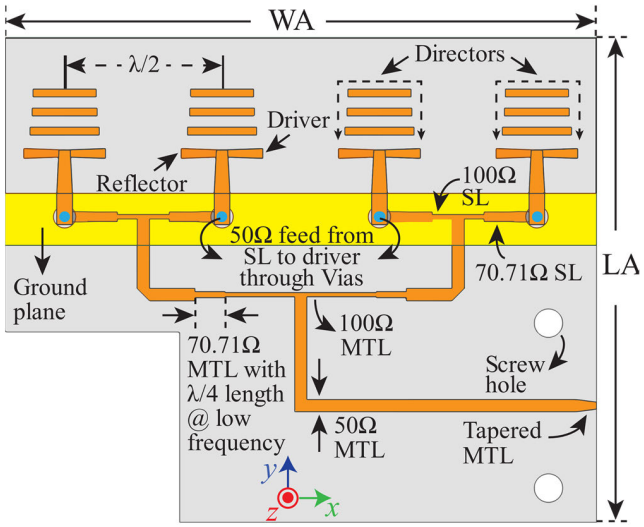

FIGURE 17. Geometrical layout of the modeled corporate feed geometrical parameters using impedance matching theory [23]. The width W_A is 34.2 mm and the length L_A is 28 mm.

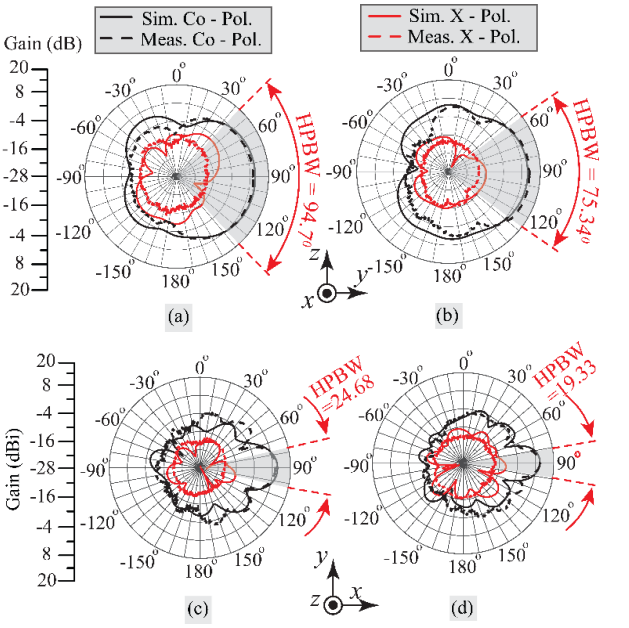

FIGURE 18. Comparison of the simulated and measured far-field radiation patterns along with Co – and Cross (X) – polarization components (a) H – plane at 17 GHz, (b) H – plane at 21 GHz, (c) E – plane at 17 GHz, and (d) E – plane at 21 GHz.

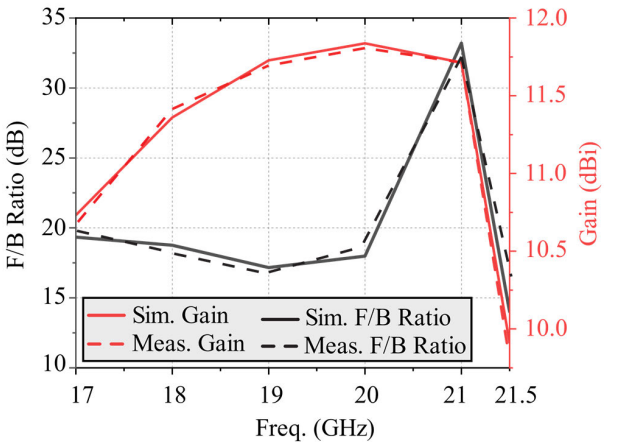

FIGURE 19. Comparison between simulated and measured boresight Gain (dBi) and F/B ratio (dB) of 1 × 4 array over the entire band of interest.

H-planes are below −16 dBi. The HPBW in the H-Plane (XZ – elevation) is broader as compared to the E-Plane (XY-azimuth), The broader HPBW of 75.34° at 21 GHz in the H-Plane is the result of EM radiations due to capacitive coupling in lateral direction.

However, a narrow HPBW of 19.33° at 21 GHz in the E-Plane is attributed to the array configuration and beam forming characteristics of the half wavelength E plane antenna array.

The achievement of wide HPBW in the H- plane as observed in the comparison of simulated and measured results further validates the employability of the proposed BCYP array in beam scanning applications in wide areas.

Moreover, a comparison between simulated and measured F/B ratio along with the boresight gain values are also plotted in Figure 19. The incorporation of the strip-line feed ensured less radiation leakage and the broadside coupling of Yagi pair also confines the radiations for the high F/B ratio. Gain reduction at the higher frequency can be observed at the upper limit of the frequency band as electric lengths of the structure change beyond the optimized ranged. A sudden gain drop beyond 21 GHz is also attributed to the pronounced dielectric and conductor losses at higher frequencies and change in the broadside coupling.

VI. DISCUSSION AND COMPARISON WITH THE MULTILAYER DESIGNS AVAILABLE IN THE LITERATURE

Finally, a detailed comparison between the existing planar and multilayer Yagi with the proposed BCYP and its array is

TABLE 2. Comparison of the proposed BCYP antenna with relevant designs from the literature.

Ref.	Fractional Bandwidth (Min [GHz]-Max [GHz]).	Gain (min[dBi]-Max[dBi])	Maximum F/B ratio (dB)	HPBW (°)	Dimensions (L-W-h) ($at\ \lambda_h$)	No. of director elements
[5]	4.25 % 57.5 – 60	8 - 11	NA	55 at 60 GHz	1.3 × 1.3 × 0.68	5
[6]	27 % 3.65 – 4.79	8.56 – 12.31	14.5	60 at 3.7 GHz	1.27 × 1.43 × 0.08	3
[7] Design # 1	13.79 % 5.4 – 6.2	4.5 – 12	NA	70 at 5.8 GHz	1.65 × 1.65 × 0.6	4
[7] Design # 2	4.36 % 5.6 – 5.85	8.1 - 11.66	NA	60 at 5.8 GHz	0.97 × 0.97 × 1.17	4
[9]	12.31 % 26.3 – 29.75	2.64 - 5.51	14.51	121 at 28 GHz	0.5 × 0.5 × 0.07	1
[10]	102.85 % 3.4 – 10.6	8 - 13	NA	NA	2.12 × 2.12 × 1.16	8
[12]	16.66 % 22 - 26	9 - 11	15.0	40 at 22 GHz	3.36 × 2.51 × 0.01	5
[24]	17.71 % 21.1 – 25.2	5 - 8	20.0	40 at 24.5 GHz	3.26 × 4.87 × 0.01	5
This work	15.78 % 17.27 – 20.23	7.21 – 7.82	17.59 at 17.5 GHz	90.38 at 17.5 GHz	0.8 × 0.54 × 2	3

TABLE 3. Comparison of proposed 1 × 4 element BCYP array with relevant array designs from the literature.

Ref.	Fractional Bandwidth (Min [GHz]-max [GHz]).	Gain (min[dBi]-Max[dBi])	Maximum F/B ratio (dB)	HPBW (°)	Dimensions (L-W-h) ($at\ \lambda_h$)	Antenna elements in Array
[5]	10.52 % 56.7 - 63	14 - 19	NA	60 at 60 GHz	5.88 × 5.04 × 0.5	4 × 4
[9] Design # 1	15.49 % 25.9 – 30.25	9.55 – 9.98	25.50	114 at 28 GHz	2.01 × 0.85 × 0.07	1 × 4
[9] Design # 2	16.82 % 25.85 – 30.6	8.98 – 9.66	19.0	112 at 28 GHz	2.04 × 0.86 × 0.076	1 × 4
[11]	8.39 % 30.8 – 33.5	7 - 10.7	15	75 at 31.7 GHz	1.45 × 0.86 × 0.02	1 × 4
[12]	12.76 % 22 - 25	11.5 - 13	20	50 at 24 GHz	3.23 × 4.83 × 0.01	1 × 2
This work	26.63 % 16.53 – 21.61	10.73 – 11.83	33.20 @ 21 GHz	94.7 at 17 GHz	2.46 × 2.01 × 0.09	1 × 4

carried out in Table 2 and Table 3, respectively. The literature comparison explains that the proposed BCYP antenna having a compact size offers additional features of wide bandwidth, wide HPBW in the H-plane, high F/B ratio, and high gain. Additionally, the literature comparison between the proposed BCYP array with the already available array design shown in Table 3 explains the wide-angle beam scanning capabilities as compared to the existing designs. A 4 × 4 array designed at 56.7 GHz – 63 GHz in [5] offers a high gain of 14 dBi – 19 dBi having HPBW of 60° at 60 GHz. However, the proposed four element BCYP array designed at 16.53 GHz – 21.61 GHz offers a wider HPBW of 94.7° at 17 GHz.

Similarly, the other four element Yagi arrays proposed in [9] and [11] offer a gain of less than 10.7 dBi. Contrarily, the proposed BCYP array offers a higher gain of 11.83 dBi at 20 GHz. The proposed array offers the highest F/B ratio of 33.20 dB as compared to the other array design compared in Table 3. These performance parameters of the proposed BCYP antenna and its array complement the requirement of airborne communication of scanning and surveillance.

VII. CONCLUSION

In this paper, a modified printed Yagi antenna in a multilayer configuration is proposed for Ku Band wide beam scanning applications. A pair of Yagi elements has been placed on different substrate layers and capacitive broadside coupling between them has been introduced for performance enhancement. The antenna structure has been fed through a

strip-line section buried in the middle layer. The proposed configuration significantly reduces radiation leakages and consequently improves antenna gain and F/B ratio as compared to a standard printed Yagi antenna. The unit BCYP antenna has been extended into a 1×4 element E-plane array formation for further gain enhancement. A wide impedance bandwidth of 5.08 GHz has been achieved for the array design. A high F/B ratio of approximately 33.2 dB with low cross-polarization level of less than -16 dBi has been successfully achieved. The array offers a gain of 11.83 dBi at 20 GHz. The design produces a much wider HPBW in the H-plane. For the single element, the H plane HPBW was measured to be 90.3° and for array configuration, the H plane HPBW was measured to be 94.7°. Thus the HPBW is not reduced but the boresight gain has been increased from 7.82 dBi for a single element to 11.83 dBi in the array formation. The wide beamwidth features with high gain and lower radiation leakages make this design an ideal candidate for cellular communication as well as for airborne surveillance and scanning applications.

ACKNOWLEDGMENT

This research work was supported by the Researchers Supporting Project, King Saud University, Riyadh, Saudi Arabia under grant RSPD2023R868. A part of this project was also completed under National Research Program for Universities (NRPU) offered by Higher Education Commission (HEC) of Pakistan (project # 8196).

REFERENCES

[1] P. Mei, S. Zhang, and G. F. Pedersen, "A low-cost, high-efficiency and full-metal reflectarray antenna with mechanically 2-D beam-steerable capabilities for 5G applications," *IEEE Trans. Antennas Propag.*, vol. 68, no. 10, pp. 6997–7006, Oct. 2020.

[2] C. Hua, Z. Shen, and J. Lu, "High-efficiency sea-water monopole antenna for maritime wireless communications," *IEEE Trans. Antennas Propag.*, vol. 62, no. 12, pp. 5968–5973, Dec. 2014.

[3] X. Chen, L. Yang, J.-Y. Zhao, and G. Fu, "High-efficiency compact circularly polarized microstrip antenna with wide beamwidth for airborne communication," *IEEE Antennas Wireless Propag. Lett.*, vol. 15, pp. 1518–1521, 2016.

[4] S. D. Targonski, R. B. Waterhouse, and D. M. Pozar, "Design of wideband aperture-stacked patch microstrip antennas," *IEEE Trans. Antennas Propag.*, vol. 46, no. 9, pp. 1245–1251, Sep. 1998.

[5] O. Kramer, T. Djerafi, and K. Wu, "Very small footprint 60 GHz stacked Yagi antenna array," *IEEE Trans. Antennas Propag.*, vol. 59, no. 9, pp. 3204–3210, Sep. 2011.

[6] Y. Liu, H. Liu, M. Wei, and S. Gong, "A novel slot Yagi-like multilayered antenna with high gain and large bandwidth," *IEEE Antennas Wireless Propag. Lett.*, vol. 13, pp. 790–793, 2014.

[7] O. Kramer, T. Djerafi, and K. Wu, "Vertically multilayer-stacked Yagi antenna with single and dual polarizations," *IEEE Trans. Antennas Propag.*, vol. 58, no. 4, pp. 1022–1030, Apr. 2010.

[8] I.-J. Hwang, H.-W. Jo, J.-W. Kim, G. Kim, J.-W. Yu, and W.-W. Lee, "Vertically stacked folded dipole antenna using multi-layer for mm-wave mobile terminals," in *Proc. IEEE Int. Symp. Antennas Propag. USNC/URSI Nat. Radio Sci. Meeting*, Jul. 2017, pp. 2579–2580.

[9] I.-J. Hwang, B. Ahn, S.-C. Chae, J.-W. Yu, and W.-W. Lee, "Quasi-Yagi antenna array with modified folded dipole driver for mmWave 5G cellular devices," *IEEE Antennas Wireless Propag. Lett.*, vol. 18, no. 5, pp. 971–975, May 2019.

[10] K. Wan, C. Xie, Y. Zheng, J. Yin, and J. Yang, "A multilayer stacked UWB Yagi antenna," in *Proc. Int. Symp. Antennas Propag. (ISAP)*, 2017, pp. 1–2.

[11] G. R. DeJean and M. M. Tentzeris, "A new high-gain microstrip Yagi array antenna with a high front-to-back (F/B) ratio for WLAN and millimeter-wave applications," *IEEE Trans. Antennas Propag.*, vol. 55, no. 2, pp. 298–304, Feb. 2007.

[12] R. A. Alhalabi and G. M. Rebeiz, "High-gain Yagi–Uda antennas for millimeter-wave switched-beam systems," *IEEE Trans. Antennas Propag.*, vol. 57, no. 11, pp. 3672–3676, Nov. 2009.

[13] R. Collin, "The optimum tapered transmission line matching section," *Proc. IRE*, vol. 44, no. 4, pp. 539–548, Apr. 1956.

[14] H. N. Awl, Y. I. Abdulkarim, L. Deng, M. Bakir, F. F. Muhammadsharif, M. Karaaslan, E. Unal, and H. Luo, "Bandwidth improvement in bow-tie microstrip antennas: The effect of substrate type and design dimensions," *Appl. Sci.*, vol. 10, no. 2, p. 504, Jan. 2020.

[15] Y.-D. Lin and S.-N. Tsai, "Coplanar waveguide-fed uniplanar bow-tie antenna," *IEEE Trans. Antennas Propag.*, vol. 45, no. 2, pp. 305–306, Feb. 1997.

[16] Y.-D. Lin and S.-N. Tsai, "Analysis and design of broadside-coupled striplines-fed bow-tie antennas," *IEEE Trans. Antennas Propag.*, vol. 46, no. 3, pp. 459–460, Mar. 1998.

[17] X. Gang, "On the resonant frequencies of microstrip antennas," *IEEE Trans. Antennas Propag.*, vol. 37, no. 2, pp. 245–247, 1989.

[18] G. Kumar and K. P. Ray, *Broadband Microstrip Antennas*. Norwood, MA, USA: Artech House, 2003.

[19] W. L. Stutzman and G. A. Thiele, *Antenna Theory and Design*, 2nd ed. New York, NY, USA: Wiley, 1998.

[20] *ANSYS HFSS Software*. Accessed: Sep. 15, 2023. [Online]. Available: http://www.ansoft.com/products/hf/hfss/

[21] Accessed: Aug. 29, 2023. [Online]. Available: https://www.hasco-Inc.com/connectors/end-launch-connectors/1092-01a-5-2-92mm-40ghz-female-end-launch-standard-profile/

[22] Accessed: Sep. 1, 2023. [Online]. Available: http://www.ainfoinc.com

[23] K. Ding and A. A. Kishk, "Multioctave bandwidth of parallel-feeding network based on impedance transformer concept," *IEEE Trans. Antennas Propag.*, vol. 67, no. 4, pp. 2803–2808, Apr. 2019.

[24] A. Dhouib, M. G. Stubbs, and M. Lecours, "Experimental and numerical analysis of a microstrip/stripline-coupling scheme for multi-layer planar antennas," in *Proc. IEEE Antennas Propag. Soc. Int. Symp. URSI Nat. Radio Sci. Meeting*, 1994, pp. 1718–1721.

MUHAMMAD NASIR received the B.S. and M.S. degrees in electrical engineering from COMSATS University Islamabad (CUI), Pakistan, in 2015 and 2020, respectively.

He is currently a Junior Research Officer with Air University, Islamabad, Pakistan. His research interests include multilayer antennas array, frequency selective surfaces, reflect array antennas, and reconfigurable antennas.

ADNAN IFTIKHAR (Senior Member, IEEE) received the B.S. degree in electrical engineering (telecommunication) from COMSATS University Islamabad (CUI), Islamabad, Pakistan, in 2008, the M.S. degree in personal mobile and satellite communication from the University of Bradford, Bradford, U.K., in 2010, and the Ph.D. degree in electrical and computer engineering from North Dakota State University (NDSU), Fargo, ND, USA, in 2016.

He is currently an Assistant Professor with the Department of Electrical Engineering, CUI, and on a postdoctoral study leave. He is also a Marie Skłodowska-Curie Fellow and a Research Executive with Hacettepe University, Ankara, Turkey, where he is researching on flexible substrate for antenna designing in biomedical and wearable applications. He has authored or coauthored 85 journals and conference publications. He was also a recipient of various national and international fundings. He has established various RF research facilities with CUI. He has been actively engaged as a reviewer of RF and antenna related international journals. His research interests include reflectarray antennas, multilayer antennas, wearable biomedical antennas, frequency selective surfaces, and metamaterial absorbers.

SYED MUZAHIR ABBAS (Senior Member, IEEE) received the B.Sc. degree in electrical (telecommunication) engineering from the COMSATS Institute of Information Technology (CIIT), Islamabad, Pakistan, in 2006, the M.Sc. degree in computer engineering from the Center for Advanced Studies in Engineering (CASE), Islamabad, in 2009, and the Ph.D. degree in electronics engineering from Macquarie University, North Ryde, NSW, Australia, in 2016. He has been a Transmission Engineer with Alcatel-Lucent, Pakistan, a RF Engineer with CommScope, Australia, and a Senior Antenna Design Engineer and a Senior Principal Engineer with Benelec Technologies, Australia. He has lectured various courses with CIIT, Islamabad, and Western Sydney University, Macquarie University, and The University of Sydney, Australia. Currently, he is a Lead Antenna Design Engineer with GME, Australia. He has been a Visiting Researcher with the ElectroScience Laboratory, The Ohio State University, USA, and Queen Mary University of London, U.K. His research interests include base station antennas, 5G antennas, mmWave antennas, 3D printed technology, metamaterials and metasurfaces, high impedance surfaces (HIS), frequency selective surfaces (FSS), electromagnetic bandgap structures (EBG), artificial magnetic conductor (AMC), beam steering, UWB, multiband antennas, flexible/embroidered antennas, CNT yarns, CNT/graphene-based antennas, reconfigurable antennas/electronics, the development of antennas for UWB, VHF, UHF, and WBAN applications. He has also received several prestigious awards and fellowships, including 2020 IEEE 5G World Forum Best Paper Award, 2019 IEEE NSW Outstanding Young Professional Award, 2018 Young Scientist Award (Commission B—Field and Waves) from the International Union of Radio Science (URSI), 2013 CSIRO Postgraduate Fellowship, 2012 iMQRES Award for the Ph.D. degree, and Research Productivity Awards from CIIT, in 2012 and 2010.

RASHID SALEEM received the B.S. degree in electronic engineering from the Ghulam Ishaq Khan Institute of Engineering Sciences and Technology, Pakistan, in 1999, the M.S. degree from the Center for Advanced Studies in Engineering, UET Taxila, Pakistan, in 2006, and the Ph.D. degree from The University of Manchester, in 2011.

He pursued a career in the telecommunication industry for several years while continuing education. In the Ph.D. degree, he was with the Microwave and Communication Systems Research Group under the supervision of Prof. Anthony (Tony) K. Brown and the Head of the School of Electrical and Electronic Engineering, The University of Manchester. He worked on antennas, channel modeling, and interference aspects of ultra-wideband systems during the Ph.D. degree and was also a member of a Team Designing and Testing Arrays for the Square Kilometer Array Project. Currently, he is a tenured Associate Professor with the University of Engineering and Technology (UET) Taxila, Pakistan, where he is supervising several postgraduate students and heading the Microwaves, Antennas and Propagation (MAP) Research Group. His research interests include antennas, angle-of-arrival-based channel modeling, microwave periodic structures, and metamaterials.

MUHAMMAD FARHAN SHAFIQUE (Senior Member, IEEE) received the M.S. degree in high-frequency communication systems from the University of Paris East Marne-La-Vallee, Paris, France, in 2005, and the Ph.D. degree in electronic and communication engineering from the University of Leeds, Leeds, U.K., in 2010. His research interests include multilayer microwave device fabrication, RF antenna, and filters. From 2007 to 2010, he was a part of the team that constructed a £1M low temperature co-fired ceramics (LTCC) and microwave fabrication facility with the University of Leeds. He pioneered a world-leading laser micromachining technology for LTCC used in RF circuits. He is currently a Professor with COMSATS University Islamabad, Pakistan, and in-charge of the research center (CAST), where he founded the Microwave Components and Devices (MCAD) Research Group. He has also established a variety of research facilities in the field of RF engineering, including five state-of-the-art laboratories. He has more than 100 peer-reviewed articles on his credit. He is also a reviewer of various international journals and conferences.

MOATH ALATHBAH received the Ph.D. degree from Cardiff University, U.K. He is currently an Assistant Professor with King Saud University, Saudi Arabia. His research interests include the development of photoelectronic, integrated electronic active and passive discrete devices, the design, fabrication, and characterization of MMIC, RF and THz components, smart antennas, microstrip antennas, microwave filters, meta-materials, 5G antennas, MIMO antennas miniaturized multiband antennas/wideband, and microwave/millimeter components using micro and nano technology.